

Magnetization Induced Second Harmonic Generation from Ultrathin Metallic Multilayers

R. VOLLMER, H. REGENSBURGER, Y. Z. WU, and J. KIRSCHNER

Max-Planck-Institut für Mikrostrukturphysik, Weinberg 2, D-06120 Halle/Saale, Germany

(Received July 10, 2001; in revised form August 20, 2001; accepted August 30, 2001)

Subject classification: 68.65.Fg; 75.70.Ak; 78.20.Ls; S1.2; S1.3

The article reviews recent measurements using the Magnetization induced Second Harmonic Generation (MSHG) from ultrathin metallic films and multilayers. Emphasis is put on the high surface and interface sensitivity and the influence of ‘quantum well states’ (QWS). With the example of a Ni/Cu/Ni/Cu(001) multilayer structure we show that there is a net (magnetic) contribution from the symmetrically buried lower Ni layer because of the presence of QWS in the Cu spacer layer, which makes the observation of antiferromagnetic coupling in the Ni/Cu/Ni/Cu(001) structure possible with MSHG.

1. Introduction

The magneto-optical Kerr effect (MOKE) has been widely used in the investigation of, for example, the magnetic properties of ultrathin films to determine thickness dependence of the Curie temperature of ultra thin layers [1], magnetic anisotropy energies and reorientation transitions [2, 3], interlayer coupling [4, 5], or adsorbate induced magnetic phase transitions [6]. MOKE measurements are fast and have a high sensitivity, so that a monolayer of ferromagnetic material can be easily detected. They require no special sample treatment and can be used to measure samples in UHV environments.

The application of MOKE to ultrathin films sometimes is named *surface* magneto-optical Kerr effect (SMOKE) [7]. However, the measured Kerr signal is an average over the entire layer stack within the penetration depth of the light of several 10 nm for metallic films. There is no special surface or interface sensitivity of MOKE. Often the magnetic properties at surfaces and interfaces are different from those of the interior of the magnetic film. In MOKE measurements these effects are largely masked by the Kerr signal from the interior of the films.

This drawback of MOKE can be avoided by using the magneto-optical effects in the frequency doubled light. Optical second harmonic generation (SHG) has been developed as a sensitive method to probe surface and interface structures [8]. For centrosymmetric materials SHG is forbidden in the bulk within the electric dipole approximation and therefore the second harmonic (SH) light is generated near the surface or interface, where the inversion symmetry is necessarily broken. The SHG arises from a non-linear polarization generated by an intense incident light field:

$$P_i(2\omega) = \chi_{ijk}^{(2)} E_j(\omega) E_k(\omega) \quad (1)$$

with $\chi^{(2)}$ the third rank tensor of the second order nonlinear susceptibility. There are higher order contributions to $\mathbf{P}(2\omega)$ like the electric quadrupole or magnetic dipole contributions, which can be of sizable magnitude [9]. However, in many cases they were found to be negligible [10]. In highly symmetric cases the coordinate system can be

chosen such that only a few elements $\chi^{(2)}$ are nonzero. For the isotropic case or for the (001) surface of a cubic crystal there are $\chi_{zxx}^{(2)} = \chi_{zyy}^{(2)}$, $\chi_{xzx}^{(2)} = \chi_{yzy}^{(2)}$, and $\chi_{zzz}^{(2)}$, all generating p-polarized second harmonic (SH) light.

Magneto-optical effects in the SHG from surfaces have been discussed in theoretical papers of Pan et al. [11] and Hübner and Bennemann [12] and have been demonstrated experimentally soon after [13–15]. Meanwhile a large number of publications have proven MSHG as a valuable tool for the investigation of magnetism at surfaces and interfaces [16–30].

In the presence of a magnetization \mathbf{M} $\chi^{(2)}$ becomes a function of \mathbf{M} , $\chi^{(2)} = \chi^{(2)}(\mathbf{M})$, and the symmetry of the surface and interfaces is further reduced. Consequently more tensor elements become nonzero [11]. Note that the magnetization as an axial vector does not lift the inversion symmetry in the bulk. In highly symmetric cases, i.e. if the magnetization lies in a mirror plane or the surface has a two-fold axis, all tensor elements $\chi_{ijk}^{(2)}$ can be classified as being either even or odd with respect to the reversal of the magnetization. Therefore all the odd and all the even tensor elements can be combined into one effective *nonmagnetic* and one effective *magnetic* tensor element with the properties

$$\chi_{nm}^{(2)}(\mathbf{M}) = \chi_{nm}^{(2)}(-\mathbf{M}); \quad \chi_m^{(2)}(\mathbf{M}) = -\chi_m^{(2)}(-\mathbf{M}). \quad (2)$$

(In this paper, it is always assumed that the Fresnel factors are included in the $\chi_{nm}^{(2)}$ or $\chi_m^{(2)}$.)

For highly symmetric cases one can distinguish three basic Kerr geometries similar to the case of MOKE: *polar*, if the magnetization is perpendicular to the surface, *longitudinal*, if the magnetization is parallel to the surface and in the optical plane. In these two cases $\chi_m^{(2)}$ generates an s-polarized SH light component for s- as well as for p-polarized incident light. Since the SH light generated by $\chi_{nm}^{(2)}$ is always p-polarized in these cases, a rotation and an ellipticity change of the SH light results. For the magnetization in the surface plane, but perpendicular to the optical plane, $\chi_m^{(2)}$ generates p-polarized SH light for s- and p-polarized incident light. Therefore an *intensity change* in the total SH light is observed.

2. Experiment

The intensity ratio of SH light from metal surfaces to fundamental light is typically of the order of 10^{-12} to 10^{-15} . For our experiments we focused the light of a Ti-sapphire laser ($\lambda = 720\text{--}950$ nm, 80 fs pulse width, repetition rate 80 MHz) onto the Cu(001) sample in an UHV chamber (angle of incidence is about 38° , spot diameter about $25\text{--}100$ μm , peak fluence below 2 mJ/cm²). The SH light is detected by a photomultiplier using lock-in technique. The fundamental light is blocked by a combination of interference and colored glass filters. For the longitudinal and polar geometry a calcite polarizer is placed in the outgoing beam path. The sample is magnetized by a dipole magnet creating a field component perpendicular to the film as well as parallel to the (110) azimuth direction.

In the transverse geometry the SH light intensity $I(2\omega, \pm\mathbf{M})$ for the magnetization in opposite directions is measured. It is useful to define an asymmetry

$$A = \frac{I(2\omega, \mathbf{M}) - I(2\omega, -\mathbf{M})}{I(2\omega, \mathbf{M}) + I(2\omega, -\mathbf{M})} = \frac{2R}{1 + R^2} \cos \phi, \quad (3)$$

with $R = |\chi_m^{(2)}/\chi_{nm}^{(2)}|$ and ϕ the phase angle between $\chi_m^{(2)}$ and $\chi_{nm}^{(2)}$. For the longitudinal and polar geometry, the asymmetry after the analyzer set at an angle α with respect to the optical plane can be written as

$$A(\alpha) = \frac{2R \tan \alpha}{1 + R^2 \tan^2 \alpha} \cos \phi. \tag{4}$$

By measuring $A(\alpha)$ it is therefore possible to determine both, R and ϕ in this geometry.

3. Surface Sensitivity of MSHG

The symmetry considerations mentioned in the introduction do not give an estimate about the effective thickness of the surface or interface, in which the SH light is generated. To answer this question, wedge-like ferromagnetic films have been grown by MBE onto a Cu(001) substrate [19, 24, 28, 31].

Figure 1 shows the SH intensity from ultrathin ferromagnetic layers of Fe, Co, and Ni on Cu(001) as function of the thickness of the ferromagnetic layer. The easy axis of magnetization of ultrathin Fe layers on Cu(001) is perpendicular to the surface plane and for Co and Ni it is along the $\langle 110 \rangle$ azimuth direction in the surface plane. Therefore the SH measurements from the Fe wedge were taken in the polar geometry and for Co and Ni in the transverse geometry.

In all three cases the SH intensity increases very rapidly with the ferromagnetic layer thickness and reaches a maximum already at about 2 monolayers (ML). This immediately shows that the effective thickness around the surface and the transition metal (TM)–Cu interface, in which the SH light is generated, is only of the order of 1–2 ML.

(The SH light intensity from the bare Cu(001) surface is quite low, because the photon energy is below the threshold of one-photon d-electron excitation). The same rapid increase can be seen in the SH asymmetry shown in the bottom row of Fig. 1: The asymmetry remains zero

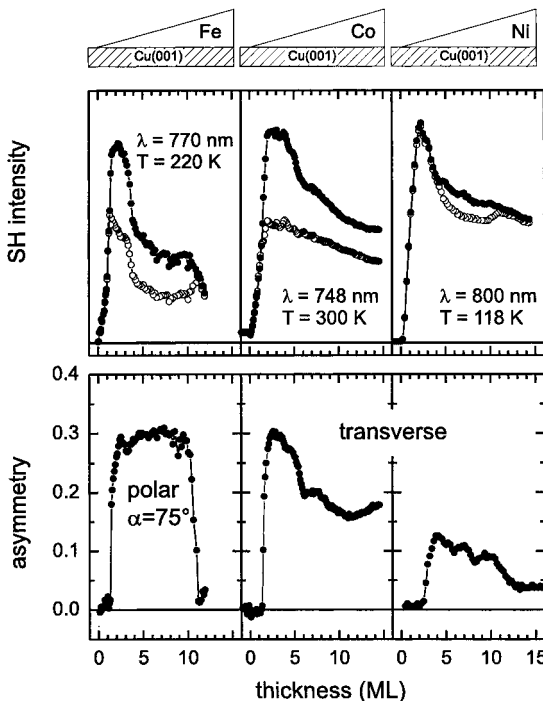


Fig. 1. SH intensity from Fe-, Co-, and Ni-wedges grown on Cu(001) (left to right, top row). Open and solid circles indicate the SH intensity for the magnetization in opposite direction. In the bottom row the corresponding SH asymmetries are shown. For Fe the measurements were taken in the polar geometry with the analyzer set to an angle of $\alpha = 75^\circ$ with respect to the incident plane. For Co and Ni the transverse geometry was used. The incident plane is parallel to the $[110]$ azimuth in all cases

until at about 1.5 ML (for Fe and Co) the film orders ferromagnetically and reaches within one ML a maximum as well. Therefore, the magnetization induced part of the SHG is essentially as surface/interface sensitive as the nonmagnetic part. The onset of ferromagnetic order in the case of the Ni film is somewhat delayed with respect to the other films even at 118 K because of the strong reduction of the Curie temperature for ultrathin Ni films.

The SH light intensity does not remain constant after the initial fast rise. There are several reasons for that: (i) In the case of Fe the structure of the film changes from the so called ‘fct’ phase, a heavily distorted fcc structure with an enlarged interlayer spacing and a 1×4 or 1×5 reconstruction, to the ‘fcc’ phase with a reduced interlayer spacing [6, 32–34]. The SH intensity drops by a factor of 2 going from the fct phase to the fcc phase. In the asymmetry this phase transition is not visible presumably because most of the magnetization induced part of the SH light is generated at the surface and all contributing tensor elements of $\chi^{(2)}$ are affected in the same way. (ii) There are no structural changes in the Co- and Ni- film in the displayed thickness range up to 10 ML¹). However, the electronic structure of ultrathin films change with their thickness. Particularly important are those states, which are (partially) bound to the film, the so called quantum well states (QWS). The long period variations in the SH intensity are caused by these QWS. This will be further discussed in one of the following sections. (iii) Especially in the data for the Co wedge there are weak 1 ML period oscillations visible in the SH intensity. These are caused by the morphology changes during the growth and will be discussed in the next section.

4. The Influence of Surface Roughness

Fe-, Co-, and Ni-films grow in a nearly layer-by-layer mode, i.e. the growth proceeds by nucleation, growth (up to a size of about 5–10 nm in diameter at 300 K [35]), and then coalescence of islands until the layer is (almost) completely filled before nucleation of island in the next layer occurs. Therefore the surface morphology undergoes a periodic change from a nearly flat surface to an island covered surface with a larger number of step edge atoms and then back to the flat surface. This change of the roughness can be monitored during the growth by, for example, medium energy electron diffraction (MEED) as shown in Fig. 2a for the case of Co growth on Cu(001) at 300 K. Except for the first ML, where the Co grows partially in a double layer growth mode the MEED intensity shows a 1 ML period oscillation due to the oscillating roughness of the surface. The same kind of oscillations can be seen in the SH light as shown in Fig. 2 as solid line for p-polarized incident light and p-polarized outgoing SH light. To emphasize the oscillations, the difference of the original curve and a smooth curve, the average over 50 datapoints, is displayed as open symbols as well. Since the wavelength of the light is much larger than this atomic scale roughness, this effect cannot be attributed to a scattering or interference effect as in the case of MEED but must be attributed to electronic changes at the step edges of the islands with a $\chi^{(2)}$, which differs from that of the flat surface.

¹) There is a spin-reorientation transition at a Ni thickness of about 11 ML, where the easy axis of magnetization rotates from in-plane to normal to the surface. However, the applied external magnetic field of about 150 Oe rotates the magnetization somewhat from the perpendicular direction. Therefore, the asymmetry does not drop to zero at 11 ML.

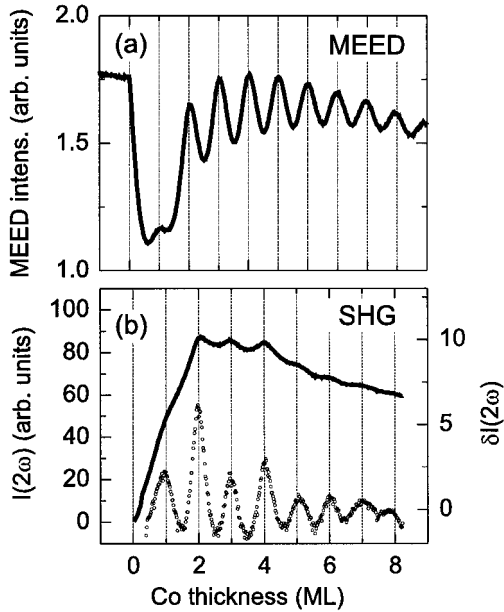


Fig. 2. Comparison of a) the MEED intensity and b) the SH light intensity $I(2\omega)$ for $p_{in}p_{out}$ polarization in the longitudinal geometry monitored during the deposition of the Co layer. The open symbols in b) (corresponding to the right scale) display the difference of the SH intensity and the average over 50 points from the solid curve. $\lambda = 790$ nm

A magnetic field parallel to the optical plane (longitudinal geometry) was applied. Therefore the p-polarized SH light is generated by the nonmagnetic tensor elements of $\chi^{(2)}$ only. The effect of the oscillating step density is also visible in the $\chi_m^{(2)}$. The effect is too small to be visible directly in the s-polarized SH light in the longitudinal geometry, where only magnetic tensor elements contribute. However, for s-polarized incident light in the transverse geometry the average SH intensity does not show the one monolayer oscillations but only the asymmetry proving that this oscillatory component comes exclusively from $\chi_m^{(2)}$ [24, 36].

5. Quantum Size Effects

While atomic scale roughness results in only small changes in the SHG, the influence of QWS can be very large and must be considered in most cases for a correct interpretation of the (M)SHG data. In metallic systems there exists no absolute band gap. However, for a fixed wave vector parallel to the surface, k_{\parallel} , the film may have states in certain energy regions which do not have corresponding states for the same k_{\parallel} in the substrate. Then, the wave function is localized in the film and the thickness, d , of the film imposes a quantization to the wave vector perpendicular to the film: $2k_{\perp}d + \delta_1 + \delta_2 = 2\pi n$, with $\delta_{1,2}$ the phase shifts at the two boundaries upon reflection. Even if there are corresponding states in the substrate, the k_{\perp} mismatch between film and substrate introduces a potential barrier and leads to a partial localization of the wave function in the film. To first approximation these states shift in energy with increasing film thickness according to the bulk band dispersion curve in the direction perpendicular to the film.

This thickness dependence of the energies of the QWS has been directly observed, for example, by angle resolved photo-emission of electrons in overlayers of noble metals on metallic substrates [37, 38]. Many other quantities are affected by these quantum size effects. If the substrate is ferromagnetic also magnetic properties like magnetic anisotropy [39] or MOKE spectra [40–42] are affected. The thickness dependence of the interlayer exchange coupling between two ferromagnetic layers through a paramagnetic spacer layer is also closely related to the QWS as well.

For most k_{\parallel} the oscillatory contribution of the QWS is averaged out in the observed physical quantity. The only remaining contribution comes from the neighborhood of so called extremal wave vectors, which determine the observed periodicities. In the case of MOKE these are the wave vectors where the derivative of the energy difference between initial and final state with respect to k_{\parallel} is zero. These extremal wave vectors depend on the energy of the light. There is generally more than one such vector and consequently a superposition of oscillation periods is observed. For the (001) surfaces of fcc crystals there are two groups of extremal vectors, one at the $\bar{\Gamma}$ point and on near the \bar{M} point. Because of the exchange splitting of the bands in the ferromagnetic layer the localization of the wave function in the paramagnetic film is different for spin up (majority) and spin down (minority) electrons inducing a circular magnetic dichroism, i.e. a Kerr effect in the paramagnetic layer [43]. According to the theory of Bruno et al. [43], the oscillation period is entirely determined by the (bulk-) band-structure of the paramagnet. The ferromagnetic layer only determines the amplitude and (possible) phase shifts of the oscillations. For Au/Fe/Au(001) all observed oscillation periods vs Au cover layer thickness agree very well with the predicted periods derived from a Au bulk band structure calculation [42]. The QWS oscillations should also be visible in the reflected light intensity, i.e. due to the diagonal terms of the linear susceptibility tensor $\chi^{(2)}$. However, up to now there is no experimental evidence for that.

The QWS oscillations observed in the (M)SHG [10, 15, 16, 22] are far less well understood [10, 44, 45]. Figure 3 shows the SH light intensity from Cu/FM/Cu(001) sandwich structures as function of the Cu cover layer for FM = Fe, Co, or Ni [28]. The wavelength for the three different measurements in Fig. 3 are nearly the same: 800, 790, and 800 nm, respectively. The fact that in all three cases the SH intensity drops upon coverage with a Cu cover layer can be easily explained by a symmetry argument: After coverage with Cu the electronic structure at the top and bottom buried interface of the ferromagnetic layer becomes equal and each point on the center plane of the ferromagnetic layer becomes a center of inversion. Consequently there should be no net SHG from these two interfaces, or in other words $\chi^{(2,b)} = -\chi^{(2,t)}$, with $\chi^{(2,b)}$ and $\chi^{(2,t)}$ the second order nonlinearity of the bottom and top interface, respectively. However, quantum well states in the Cu cover layer modify the electronic structure at the top interface and cause the oscillatory like behavior observed for larger Cu cover layer thickness.

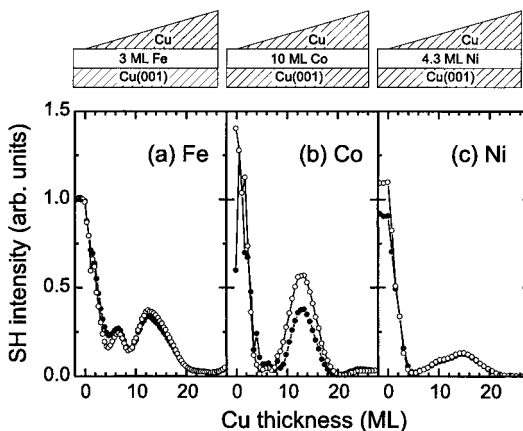


Fig. 3. SH light intensity from a) a Cu/3 ML Fe/Cu(001), b) a Cu/10 ML Co/Cu(001), and c) a Cu/4.3 ML Ni/Cu(001) multilayer structure measured with p-polarized incident light at $\lambda = 800, 790,$ and 800 nm, respectively, as function of the Cu cover layer. The magnetization for the Fe layer was mainly perpendicular to the surface, while for Co and Ni the magnetization was in the surface plane perpendicular to the optical plane. The solid and open symbols are the SH intensity for the magnetization in opposite directions. The Fe and Co samples were measured at room temperature, Ni at 123 K

In a first attempt, Luce et al. [44] presented a qualitative explanation of the observed oscillation in the SH light intensity from Cu/Fe/Cu(001) by a process similar to that used to explain the oscillations in the MOKE data: virtual two-photon transitions at the Cu/TM interface from the Cu 3d states or Fe-derived 3d states to QWS derived from the 4s bulk band of Cu at the extremal wave vectors. For photon energies around 1.3–1.7 eV, used in the experiments, the SHG from the Cu overlayer is very weak. However, due to resonance of the intermediate transition state with interface states derived from the ferromagnetic layer the signal is enhanced by almost two orders of magnitude. There is an important difference to the MOKE case: (i) There the whole paramagnetic cover layer contributes to the Kerr signal while the SHG is localized at the Cu/Fe interface (in the dipole approximation) since the intermediate Fe-derived state is localized at the Cu/Fe buried interface. (ii) An induced dichroism in the Cu cover layer is not necessary to explain the magnetization dependence of the SH intensity vs. Cu cover layer thickness curve since this dependence is already mediated by the exchange split Fe-derived intermediate state.

Figure 4 shows the wavelength dependence of the SHG vs. Cu cover layer thickness for Cu/10 ML Co/Cu(001). According to the above explanation and similar to MOKE, the period(s) should not depend on the ferromagnetic material which may only affect the amplitude and (possible) phase shifts. It is obvious from Fig. 4 that more than one period contribute. A Fourier analysis of the SH intensity curves results in a broad spectrum of periodicities around 15 ML, whose maximum does not change very much with the wavelength of the incident light. (The analysis of SH asymmetry is complicated by the large variation in the (average) SH intensity, introducing additional oscillations in the asymmetry, which do not reflect oscillations in $\chi_m^{(2)}$ [10].) This behavior is not in agreement with the above described mechanism of Luce et al., from which a strong shift to longer periods with decreasing wavelength of the incident light would be expected. However, besides the above mentioned process several other transitions may contribute to the SHG with their own periodicities: Instead of a the Cu derived 3d state

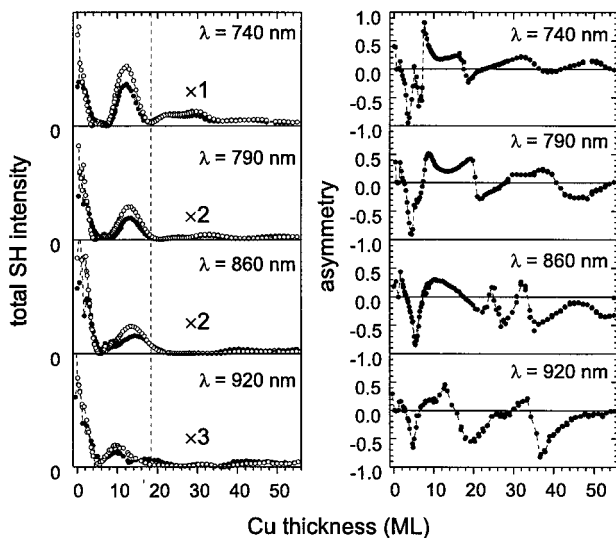


Fig. 4. SH intensity from a Cu/10 ML Co/Cu(001) multilayer as function of the Cu cover layer thickness for various wavelengths λ of the incident light. The SH intensity curves were measured in the transverse geometry. Open and solid symbols indicate measurements with the magnetization in opposite directions. The intensities are normalized against a quartz reference and scaled by the indicated factors. On the right hand panels the asymmetries calculated from the SH intensities are shown

a FM layer derived 3d interface state can act as initial state for the transition [44, 45]. Since the energy of this state is different from the energy of the Cu 3d state, the value of the extremal wave vector is changed leading to a different period in the SHG. Transitions with a quantum well state as intermediate state are possible as well [10]. In this case QWS below E_F are probed, which are completely localized inside the Cu over-layer for the minority channel [46]. Therefore they should contribute especially strongly to the oscillation in the SH light.

For all these transitions periods in the range of ≈ 3 to ≈ 9 ML are expected. However, only longer periods are observed. It was proposed that these short period oscillations are averaged out by the surface and interface roughness and only the beating frequency of two (or more) of these oscillations are observed [10]. This could explain the wavelength behavior of the main peak in the spectra in Fig. 4. However, the combination of the above mentioned processes allows almost all kinds of periods that without the precise knowledge of the energies of all contributing interface states a quantitative fit of the data is not uniquely possible.

The above mentioned considerations apply to the (001) surfaces of fcc noble metal cover layers. On (111) surfaces a different behavior was observed. In general the variations of the SHG with the cover layer thickness were found not as strong as for the (001) surfaces. In the SH intensity from Au/Co/Au(111) a single oscillation period of about 13–16 ML was observed, which does not depend on the wavelength of the light very much [22] and is always twice the period found in the linear Kerr signal [47]. In case of the (111) surface the extremal wave vector does not change much for different photon energies [47]. This may explain the weak photon energy dependence of the observed oscillation.

The fact that the SH signal shows a period twice as long as that observed in MOKE in the systems and wavelength region investigated up to now is not yet understood and may be purely accidental. The considerations made by the authors of Refs. [45, 48] that the symmetry of the QWS wave functions with respect to inversion is responsible for the observed period doubling and only QWS with odd parity are contributing, are not convincing: An isolated free standing ultrathin layer does not generate any SHG at all in the dipole approximation. Only the presence of the substrate breaks the inversion symmetry of the film and yields a net SHG. It is argued in Ref. [45] that the substrate influences the QWS only weakly and that therefore the wave functions remain “nearly” even or odd. A product of matrix elements like $\langle d_1 | \mathbf{p} | d_2 \rangle \langle d_2 | \mathbf{p} | \text{QWS} \rangle \langle \text{QWS} | \mathbf{p} | d_1 \rangle$ enters the expression for $\chi^{(2)}$, with $|d_{1,2}\rangle$ d-states, $|\text{QWS}\rangle$ quantum well states, and \mathbf{p} the momentum operator. The d-states are assumed to be “nearly” even by the authors of Ref. [45]. Then the first matrix elements in the product always nearly vanish since \mathbf{p} is odd. The two remaining matrix elements also nearly vanishes for even QWS but not for odd QWS from which the authors conclude the doubled period. However, for the case of MOKE an expression like $\langle d_1 | \mathbf{p} | \text{QWS} \rangle \langle \text{QWS} | \mathbf{p} | d_1 \rangle$ enters the linear susceptibility $\chi^{(1)}$ from which the authors have to conclude a period doubling for MOKE as well in contradiction to the experimental result.

Whether or not, and if so, why the parity of QWS plays a role for the observed oscillations in the SHG is an open question. Also the question to which extent the SHG is restricted to a region near the interfaces, if extended states like the QWS contribute, is not yet completely answered. Experimental data over a wider spectral range and a theoretical model, allowing a more quantitative comparison with the experimen-

tal data are necessary. Nevertheless, the experimental results presented above clearly show that QWS strongly influence the (M)SHG from thin films and multilayers and must be considered in the interpretation of the MSHG data.

6. Interlayer Exchange Coupling

In this section we want to discuss the MSHG from a more complex structure involving two ferromagnetic layers separated by a paramagnetic spacer layer. The example of a 6 ML Ni/ x ML Cu/6 ML Ni/Cu(001) multilayer structure shows unambiguously that it is mainly the influence of the QWS in the paramagnetic spacer layer, which generates a net contribution to the (magnetic) SHG from the symmetrically buried Ni film. While in the limit of ultrathin layers it is generally difficult to separate the SHG from individual interfaces or layers unambiguously, the magnetic contribution from the buried Ni layer can be separated quite directly, because the magnetization of the buried Ni film is aligned antiparallel for certain Cu spacer thickness due to the interlayer exchange coupling. By an external magnetic field the magnetization direction can be aligned parallel to the top Ni layer, causing only a sign change of magnetic $\chi^{(2)}$ from the two interfaces of the buried Ni layer without affecting the nonmagnetic $\chi^{(2)}$ (which are even in \mathbf{M}) or significantly the $\chi^{(2)}$ from the other interfaces.

The antiparallel coupling was first observed in Fe/Cr/Fe layers by Grünberg et al. [49]. It was found that the coupling strength oscillates with the spacer layer and occurs with almost any transition or noble metal as a spacer material [50, 51]. The interlayer exchange coupling is mediated by spin dependent confinement of quantum well states in the (paramagnetic) spacer layer [52]. To a good approximation the period(s) observed in the coupling strength are determined by extremal wave vector(s) of the bulk Fermi surface of the spacer material. Although the theories explaining the interlayer coupling and the oscillations in MOKE as function of a paramagnetic cover layer are closely related, the extremal wave vectors and therefore the observed periods are different for these two phenomena.

Figure 5a shows a hysteresis curve measured by MOKE (Kerr rotation) from a 6 ML Ni/10 ML Cu/6 ML Ni trilayer structure grown on Cu(001). Details of preparation conditions can be found in Refs. [5] and [28]. At this interlayer thickness the two Ni layers couple antiferromagnetically. To first approximation the Kerr rotation amplitude is proportional to the difference of the magnetic moment of the top and the bottom film. The Ni/Cu interface causes a stronger reduction of the magnetic moment (and of the Kerr rotation) than the Ni/vacuum interface [53]. Therefore the magnetization of the bottom film is lower than that of the top film despite the same thickness of the layers. Under an external field exceeding the coupling field (of about 80 Oe in this case) the magnetization of the bottom layer is aligned parallel to that of the top layer. The Kerr amplitude is approximately proportional to the sum of the magnetic moment per area of the top and bottom Ni film.

The hysteresis curve in the SH light intensity is shown in Fig. 5b. Because of the surface and interface sensitivity, the amplitude in the MSHG hysteresis loop cannot be a measure of the total magnetization. The measured SH intensity results from the coherent superposition of the SH light generated at all four interfaces. However, the fact that the change in the SH intensity upon reversal of the (net) magnetization at remanence differs from that at saturation, shows immediately that there is a net contribution

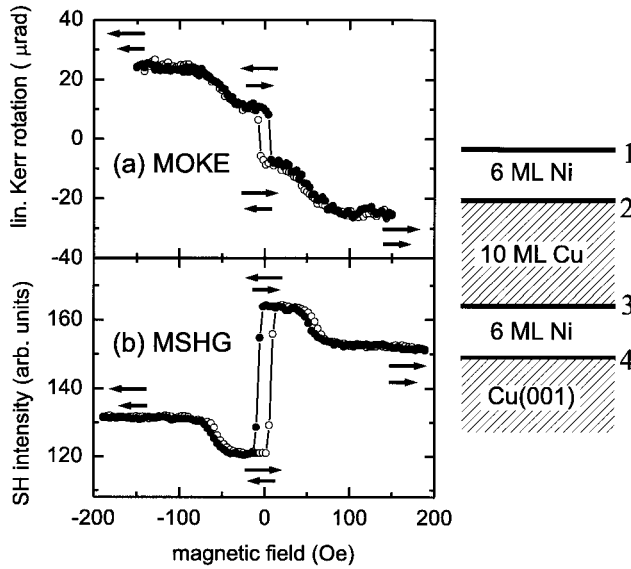


Fig. 5. Comparison of a hysteresis loop measured with a) MOKE and b) MSHG on a 6 ML Ni/10 ML Cu/6 ML Ni/Cu(001) multilayer structure with the Cu spacer layer in the antiferromagnetic coupling range. The solid (open) symbols represent the measurements with increasing (decreasing) magnetic field. The arrows indicate the direction of the upper (long arrow) and lower (short arrow) Ni film. $T = 220$ K

$\Delta\chi_m^{(2)}$ from the two interfaces of the buried Ni film. Since $\Delta\chi_m^{(2)}$ is a complex quantity, it depends on the phase difference of $\Delta\chi_m^{(2)}$ to the phase of the rest of the nonlinear magnetic and nonmagnetic susceptibility, whether $\Delta\chi_m^{(2)}$ leads to an enhancement or a reduction of the MSHG asymmetry.

In saturation, where the magnetization of the top and bottom film is aligned parallel, there should be no net SH contribution, even if we consider the influence of QWS in the Cu interlayer on the SHG, provided that the QWS are fully confined to this layer. The SH light generated by the third interface (numbered from the surface, see Fig. 5) is canceled by the SH light generated by the second interface, since each point on the center plane of the Cu interlayer is a center of inversion and the QWS are present at both interfaces. The remaining first and fourth interface would generate the same SH light intensity as a single Ni film. At remanence an additional net magnetic contribution $2\Delta\chi_m^{(2)}$ arises because of the opposite orientation of the magnetization of the bottom film. The magnetic contribution of the interfaces of the Cu interlayer does not vanish any more and the MSHG signal in remanence should depend on the thickness of the Cu interlayer.

This is indeed, what is observed. In Fig. 6a the SH asymmetry at saturation (solid circles) and remanence (open circles) are plotted as function of the Cu interlayer thickness. While at 10 ML the magnitude of the asymmetry is larger than that at saturation, it is just the opposite for a Cu interlayer thickness of 24 ML. The (average) SH intensity does not change much (less than $\pm 10\%$) as it is expected from the above model considerations (Fig. 6b). Clearly, the presence of the QWS is the main reason for the observability of the symmetrically buried Ni layer. Differences in the degree of roughness of the interfaces cannot explain the sign changes of $\Delta\chi_m^{(2)}$, since the roughness of the interfaces to the Ni film increases monotonously with the Cu interlayer thickness.

The fact that the SH asymmetry in saturation is not entirely constant is not in agreement with the model, where it was assumed that the QWS are fully confined to the Cu

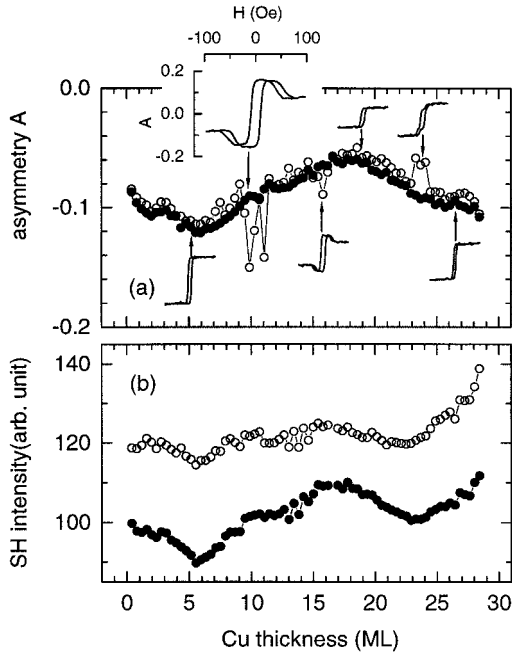


Fig. 6. a) SH asymmetry and b) intensity as function of the Cu spacer layer from a 6 ML Ni/ x ML Cu/6 ML Ni/Cu(001) wedge measured with p-polarized incident light at 200 K. The solid (open) symbols in a) indicate the asymmetry with (solid) and without (open) an externally applied field of 190 Oe

interlayer. Especially for the case of Ni/Cu/Ni, however, this is not strictly true and the QWS extend through the whole layer stack [5]. Therefore, the first and fourth interface are affected by the QWS as well, which results in the observed dependence of the asymmetry on the Cu interlayer thickness.

7. Conclusion

In conclusion we have shown that magnetization induced second harmonic generation can be a very surface and interface sensitive tool for studying ultrathin multilayers. Atomic scale roughness can be detected in the nonmagnetic and magnetic part of SHG. However, for ultrathin multilayers with nearly flat interfaces, presented in this paper, the influence of QWS are dominating. The QWS are responsible for the observability of symmetrically buried layers. Therefore the exchange coupling strength of antiferromagnetically coupled layers can be measured with MSHG. This is due to the QWS in the *nonmagnetic* interlayer.

References

- [1] R. VOLLMER, S. VAN DIJKEN, M. SCHLEBERGER, and J. KIRSCHNER, *Phys. Rev. B* **61**, 1303 (2000).
- [2] R. VOLLMER, TH. GUTJAHR-LÖSER, J. KIRSCHNER, S. VAN DIJKEN, and B. POELSEMA, *Phys. Rev. B* **60**, 6277 (1999).
- [3] S. VAN DIJKEN, R. VOLLMER, B. POELSEMA, and J. KIRSCHNER, *J. Magn. Magn. Mater.* **210**, 316 (2000).
- [4] R. SCHÄFER, *J. Magn. Magn. Mater.* **148**, 226 (1995).
- [5] Y. Z. WU, R. VOLLMER, H. REGENSBURGER, and J. KIRSCHNER, *Phys. Rev. B* **62**, 5810 (2000).
- [6] R. VOLLMER and J. KIRSCHNER, *Phys. Rev. B* **61**, 4146 (2000).
- [7] Z. Q. QIU and S. D. BADER, *J. Magn. Magn. Mater.* **200**, 664 (2000).
- [8] K. H. BENNEMANN (Ed.), *Nonlinear Optics in Metals*, Vol. 98, International Series of Monographs on Physics, Oxford University Press, New York 1998.
- [9] R. VOLLMER, M. STRAUB, and J. KIRSCHNER, *Surf. Sci.* **352/354**, 684 (1996).
- [10] R. VOLLMER, in: *Nonlinear Optics at Metallic Interfaces*, Ed. K.-H. BENNEMANN, Oxford University Press, Oxford 1998 (Chap. 2, pp. 42–131).
- [11] R.-P. PAN, H. D. WEI, and Y. R. SHEN, *Phys. Rev. B* **39**, 1229 (1989).

- [12] W. HÜBNER and K.-H. BENNEMANN, *Phys. Rev. B* **40**, 5973 (1989).
- [13] J. REIF, J. C. ZINK, C.-M. SCHNEIDER, and J. KIRSCHNER, *Phys. Rev. Lett.* **67**, 2878 (1991).
- [14] G. SPIERINGS, V. KOUTSOS, H. A. WIERENGA, M. W. J. PRINS, D. ABRAHAM, and TH. RASING, *Surf. Sci.* **287**, 747 (1993).
- [15] H. A. WIERENGA, W. DE JONG, M. W. PRINS, TH. RASING, R. VOLLMER, A. KIRILYUK, H. SCHWABE, and J. KIRSCHNER, *Phys. Rev. Lett.* **74**, 1462 (1995).
- [16] R. VOLLMER, A. KIRILYUK, H. SCHWABE, J. KIRSCHNER, H. A. WIERENGA, W. DE JONG, and TH. RASING, *J. Magn. Magn. Mater.* **148**, 295 (1995).
- [17] K. BÖHMER, J. HOHLFELD, and E. MATTHIAS, *Appl. Phys. A* **60**, 203 (1995).
- [18] R. VOLLMER, M. STRAUB, and J. KIRSCHNER, *Surf. Sci.* **352**, 937 (1996).
- [19] M. STRAUB, R. VOLLMER, and J. KIRSCHNER, *Phys. Rev. Lett.* **77**, 743 (1996).
- [20] R. VOLLMER, M. STRAUB, and J. KIRSCHNER, *J. Magn. Soc. Japan* **20**, 29 (1996).
- [21] T. M. CRAWFORD, C. T. ROGERS, T. K. SILVA, and Y. K. KIM, *Appl. Phys. Lett.* **68**, 1573 (1996).
- [22] A. KIRILYUK, TH. RASING, R. MÉGY, and P. BEAUVILLAIN, *Phys. Rev. Lett.* **77**, 4608 (1996).
- [23] K. J. VEENSTRA, A. V. PETUKHOV, A. P. DE BOER, and TH. RASING, *Phys. Rev. B* **58**, R16020 (1998).
- [24] Q. Y. JIN, H. REGENSBURGER, R. VOLLMER, and J. KIRSCHNER, *Phys. Rev. Lett.* **80**, 4056 (1998).
- [25] V. JÄHNKE, U. CONRAD, J. GÜDDE, and E. MATTHIAS, *Appl. Phys. B* **68**, 485 (1999).
- [26] F. MANDERES, K. J. VEENSTRA, A. KIRILYUK, and TH. RASING, *Appl. Phys. Lett.* **73**, 3601 (1998).
- [27] T. V. MURZINA, A. A. DEDYANNIN, T. V. MISURYAEV, G. B. KHOMUTOV, and O. A. AKTSIPETROV, *Appl. Phys. B* **68**, 537 (1999).
- [28] Y. Z. WU, R. VOLLMER, H. REGENSBURGER, X.-F. JIN, and J. KIRSCHNER, *Phys. Rev. B* **63**, 054401 (2001).
- [29] U. CONRAD, J. GÜDDE, V. JÄHNKE, and E. MATTHIAS, *Phys. Rev. B* **63**, 144417 (2001).
- [30] K. BAL, A. KIRILYUK, and TH. RASING, *J. Appl. Phys.* **89**, 4670 (2001).
- [31] R. VOLLMER, Q. Y. JIN, H. REGENSBURGER, and J. KIRSCHNER, *J. Magn. Magn. Mater.* **198/199**, 611 (1999).
- [32] P. BAYER, S. MÜLLER, P. SCHMAILZL, and K. HEINZ, *Phys. Rev. B* **48**, 17611 (1993).
- [33] S. MÜLLER, P. BAYER, C. REISCHL, K. HEINZ, B. FELDMANN, H. ZILLGEN, and M. WUTTIG, *Phys. Rev. Lett.* **74**, 765 (1995).
- [34] S. MÜLLER, P. BAYER, A. KINNE, P. SCHMAILZL, and K. HEINZ, *Surf. Sci.* **322**, 21 (1995).
- [35] A. K. SCHMID and J. KIRSCHNER, *Ultramicroscopy* **42/44**, 483 (1992).
- [36] Q. Y. JIN, H. REGENSBURGER, R. VOLLMER, and J. KIRSCHNER, *J. Appl. Phys.* **85**, 5288 (1999).
- [37] T. MILLER, A. SAMSAVAR, G. E. FRANKLIN, and T.-C. CHIANG, *Phys. Rev. Lett.* **61**, 1404 (1988).
- [38] J. E. ORTEGA, F. J. HIMPEL, G. J. MANKEY, and R. F. WILLIS, *Phys. Rev. B* **47**, 1540 (1993).
- [39] W. WEBER, A. BISCHOF, R. ALLENSPACH, C. WÜRSCH, C. H. BACK, and D. PESCIA, *Phys. Rev. Lett.* **76**, 3424 (1996).
- [40] W. R. BENNETT, W. SCHWARZACHER, and J. W. F. EGELHOFF, *Phys. Rev. Lett.* **65**, 3169 (1990).
- [41] V. GROLIER, D. RENARD, B. BARTENLIAN, P. BEAUVILLAIN, C. CHAPPERT, C. DUPAS, J. FERRÉ, M. GALTIER, E. KOLB, M. MULLOY, J. P. RENARD, and P. VEILLET, *Phys. Rev. Lett.* **71**, 3023 (1993).
- [42] Y. SUSUKI, T. KATAYAMA, P. BRUNO, S. YUASA, and E. TAMUR, *Phys. Rev. Lett.* **80**, 5200 (1998).
- [43] P. BRUNO, Y. SUZUKI, and C. CHAPPERT, *Phys. Rev. B* **53**, 9214 (1996).
- [44] T. LUCE, W. HÜBNER, and K. H. BENNEMANN, *Phys. Rev. Lett.* **77**, 2810 (1996).
- [45] T. A. LUCE, W. HÜBNER, A. KIRILYUK, TH. RASING, and K. H. BENNEMANN, *Phys. Rev. B* **57**, 7377 (1998).
- [46] P. VAN GELDERN, S. CRAMPIN, and J. E. INGLESFIELD, *Phys. Rev. B* **53**, 9115 (1996).
- [47] R. MÉGY, A. BONOUH, Y. SUZUKI, P. BEAUVILLAIN, P. BRUNO, B. LECUYER, and P. VEILLET, *Phys. Rev. B* **51**, 5586 (1995).
- [48] K. H. BENNEMANN, *J. Magn. Magn. Mater.* **200**, 679 (1999).
- [49] P. GRÜNBERG, R. SCHREIBER, Y. PANG, M. B. BRODSKY, and H. SOWERS, *Phys. Rev. Lett.* **57**, 2442 (1986).
- [50] S. S. P. PARKIN, N. MORE, and K. P. ROCHE, *Phys. Rev. Lett.* **64**, 2304 (1990).
- [51] S. S. P. PARKIN, *Phys. Rev. Lett.* **67**, 3598 (1991).
- [52] P. BRUNO, *Phys. Rev. B* **52**, 411 (1995).
- [53] X.-Y. ZHU, H. HUANG, and J. HERMANSON, *Phys. Rev. B* **29**, 3009 (1984).